Electronic Properties of the Insulating Half-Filled Hubbard Model

N. Bulut,[1] D. J. Scalapino,[2] and S. R. White[3]

[1]*Department of Physics and Materials Research Laboratory, University of Illinois at Urbana-Champaign, Urbana, Illinois 61801-3080*

[2]*Department of Physics, University of California at Santa Barbara, Santa Barbara, California 93106-9530*

[3]*Department of Physics, University of California at Irvine, Irvine, California 92717-4575*

(Received 4 March 1994)

Monte Carlo results for the frequency dependent conductivity $\sigma_1(\omega)$, the angular resolved photoemission spectral weight $A(\mathbf{p},\omega)$, and the electron momentum distribution $\langle n_\mathbf{p}\rangle$ are calculated for a half-filled Hubbard model with the on-site Coulomb interaction U equal to the bandwidth $8t$. We find that even for $U = 8t$, a spin-density-wave approximation provides a sensible description of this data and hence a useful picture of the electronic degrees of freedom in the insulating state.

PACS numbers: 79.60.Bm, 74.72.−h, 78.50.Ec

Neutron scattering experiments show that the spin degrees of freedom of the insulating cuprates are well described by an $S = 1/2$ antiferromagnetic Heisenberg model. However, the interpretation of the frequency dependent conductivity and angular resolved photoemission spectroscopy (ARPES) studies of the insulating cuprates require that the charge degrees of freedom also be included. A spin-density-wave (SDW) description provides a weak-coupling approach, in which both the collective antiferromagnetic spin fluctuation and the itinerant electronic charge degrees of freedom can be taken into account. Furthermore, Schrieffer, Wen, and Zhang [1] showed that a random phase approximation (RPA) calculation of the spin-wave spectrum in an SDW state not only gave the correct weak-coupling results, but in addition provided a sensible fit to the strong-coupling behavior.

Here we report quantum Monte Carlo (QMC) results for the conductivity, the one-electron spectral weight, and electron momentum occupation of a two-dimensional, half-filled Hubbard model with an on-site Coulomb interaction U equal to the one-electron bandwidth. Thus, we are well out of the weak-coupling regime. For these parameters, local moments are well formed and the ground state is characterized by long-range antiferromagnetic order. The frequency dependent conductivity and the single-particle spectral weight exhibit a well developed insulating gap set by the Coulomb interaction. Nevertheless, we find that the frequency dependent conductivity, the momentum dispersion, and relative spectral weights of the peaks in the single-particle spectral weight and the momentum distribution $\langle n_\mathbf{p}\rangle$ of the electrons are in good agreement with the SDW picture.

In the Hubbard model

$$H = -t\sum_{\langle i,j\rangle,s}(c_{is}^\dagger c_{js} + c_{js}^\dagger c_{is}) + U\sum_i n_{i\uparrow}n_{i\downarrow}, \qquad (1)$$

the operator $c_{is}^\dagger$ creates an electron of spin s on site i and n_{is} is the number operator for spin s and site i. For the simple near-neighbor form of the kinetic energy, the band energy $\varepsilon_\mathbf{p}$ is

$$\varepsilon_\mathbf{p} = -2t[\cos(p_x) + \cos(p_y)]. \qquad (2)$$

When U is comparable to or larger than the bandwidth $8t$, the spin degrees of freedom are well described by a spin-1/2 antiferromagnetic Heisenberg Hamiltonian with an exchange interaction $J \simeq 4t^2/U$. Here we will consider the half-filled band $\langle n_{i\uparrow} + n_{i\downarrow}\rangle = 1$ with $U = 8t$. In this case, for temperatures well below $8t$, local moments form with $\sqrt{\langle(n_{i\uparrow} - n_{i\downarrow})^2\rangle} = 0.95$. As the temperature decreases below J, antiferromagnetic correlations develop and at low temperatures the antiferromagnetic correlation length grows exponentially. For the temperature $T = 0.125t$, at which we have carried out the Monte Carlo simulations discussed below, the antiferromagnetic correlation length is larger than the 12×12 lattice we have used.

The real part of the frequency dependent $\mathbf{q} = 0$ conductivity is given by the Kubo relation

$$\sigma_1(\omega) = \mathrm{Re}\,\frac{\Lambda_{xx}(i\omega_m)}{i\omega_m}\bigg|_{i\omega_m\to\omega+i\delta} \qquad (3)$$

with

$$\Lambda_{xx}(i\omega_m) = \int_0^\beta d\tau\, e^{-i\omega_m\tau}\langle j_x(\tau)\, j_x^\dagger(0)\rangle. \qquad (4)$$

Here ω_m is a Matsubara frequency $2\pi mT$, $j_x(\tau) = \exp(H\tau)j_x\exp(-H\tau)$, and

$$j_x = -ite\sum_{is}\left(c_{is}^\dagger c_{i+xs} - c_{i+xs}^\dagger c_{is}\right). \qquad (5)$$

The current-current Green's function given in Eq. (4) is evaluated with the usual Monte Carlo method [2,3]. Note that at half filling there is no fermion sign problem. The analytic continuation in Eq. (3) is carried out using a maximum entropy procedure [4,5].

The results obtained for $\sigma_1(\omega)$ versus ω are shown as the solid curve in Fig. 1. A clear gap is seen which is consistent with the vanishing Drude weight discussed in

0031-9007/94/73(5)/748(4)$06.00

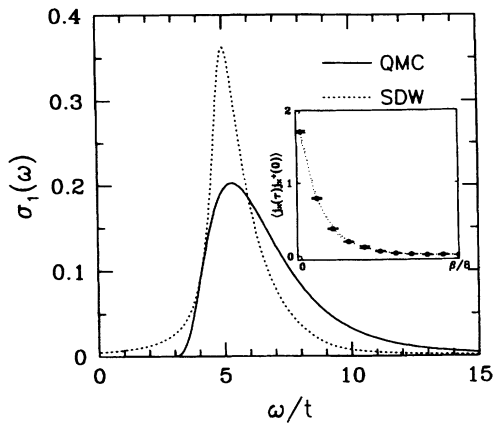

FIG. 1. Real part of the frequency dependent conductivity of a half-filled $\langle n\rangle = 1$ Hubbard model with $U = 8t$. These results were obtained on a 12×12 lattice at a temperature $0.125t$. This set of parameters will be used for all of the results discussed here. The dotted line is the mean field SDW result with $\Delta = 2.4t$. A finite broadening of $\Gamma = 0.5t$ has been used in plotting the SDW result. The inset shows the τ dependent current-current correlation function used to obtain the conductivity.

Ref. [6] and the insulating nature of the half-filled system. The dotted curve is the mean field SDW result

$$\sigma_1(\omega) = \frac{2\pi}{N}\sum_{\mathbf{p}} \sin^2(p_x)\frac{1}{2}\left(1 - \frac{\varepsilon_{\mathbf{p}}^2 - \Delta^2}{E_{\mathbf{p}}^2}\right) \times \left(\frac{1 - 2f(E_{\mathbf{p}})}{E_{\mathbf{p}}}\right)\delta(\omega - 2E_{\mathbf{p}}) \tag{6}$$

with $\Delta = 2.4t$ and the δ function broadened [7]. The zero temperature mean field SDW gap determined from

$$1 = \frac{U}{N}\sum_{\mathbf{p}} \frac{1}{2E_{\mathbf{p}}} \tag{7}$$

is equal to $3.6t$. When the RPA fluctuations are taken into account [1], Δ is reduced to $2.4t$.

The mean field result for $\sigma_1(\omega)$ given by Eq. (6) is similar to the BCS expression for a superconductor except for the change in sign of the Δ^2 term and the fact that Δ in Eq. (6) is the the spin-density-wave gap. Near threshold $\omega \simeq 2\Delta$, $\varepsilon_{\mathbf{p}}$ vanishes and the coherence factor $\frac{1}{2}[1 - (\varepsilon_{\mathbf{p}}^2 - \Delta^2)/E_{\mathbf{p}}^2]$ goes to 1. In the superconductor, this coherence factor vanishes at threshold which accounts for the absence of a peak in $\sigma_1(\omega)$ at $\omega = 2\Delta$ in the superconducting case. The f-sum rule for the Hubbard model has the form

$$\int_0^\infty d\omega\, \sigma_1(\omega) = \frac{\pi}{2}\langle -k_x\rangle \tag{8}$$

with $\langle k_x\rangle$ the average kinetic energy per site associated with hopping in the x direction:

$$\langle k_x\rangle = -t\sum_s \left\langle c_{\ell+xs}^\dagger c_{\ell s} + c_{\ell s}^\dagger c_{\ell s+xs}\right\rangle. \tag{9}$$

The Monte Carlo results give $\frac{\pi}{2}\langle -k_x\rangle = 0.77$ and the area under the solid curve in Fig. 1 showing the Monte Carlo data for $\sigma_1(\omega)$ gives 0.74. The small difference reflects the difficulty in analytically continuing the numerical data. The spin-density-wave result

$$\frac{\pi}{2}\langle -k_x\rangle = -\frac{\pi}{2N}\sum_{\mathbf{p}} \varepsilon_{\mathbf{p}}\frac{1}{2}\left(1 - \frac{\varepsilon_{\mathbf{p}}}{E_{\mathbf{p}}}\right) \tag{10}$$

gives 0.85. This approximation overestimates the size of the kinetic energy, and hence the area under $\sigma_1(\omega)$. Nevertheless, the simple spin-wave result for $\sigma_1(\omega)$ is similar to the Monte Carlo data.

In order to learn more about the one-electron properties of this system, we have calculated the single-particle spectral weight

$$A(\mathbf{p},\omega) = -\frac{1}{\pi}\operatorname{Im} G(\mathbf{p}, i\omega_n)\Big|_{i\omega_n\to\omega+i\delta} \tag{11}$$

by anaytically continuing the Monte Carlo data with the maximum entropy technique. Figure 2 shows plots of $A(\mathbf{p},\omega)$ versus ω for various momentum slices through the Brillouin zone, and Fig. 3 shows the single-particle density of states

$$N(\omega) = \frac{1}{N}\sum_{\mathbf{p}} A(\mathbf{p},\omega). \tag{12}$$

The insulating gap is clearly evident. However, it is also clear from Fig. 2 that the peak in $A(\mathbf{p},\omega)$ disperses. In Fig. 2(a), the spectral weight exhibits two peaks which disperse symmetrically about $\omega = 0$. The relative spectral weight shifts from negative to positive energies as the momentum moves from below $(\pi/2,\pi/2)$ to above this value. At the $(\pi/2,\pi/2)$ point, the spectral weight is symmetrically distributed. In an ARPES experiment, only the $\omega \le 0$ spectral weight is observable. Thus at first glance, it might appear that the peak in $A(\mathbf{p},\omega)$ passed through a "Fermi surface" as the momentum is changed from $(\pi/2,\pi/2)$ to $(2\pi/3,2\pi/3)$. However, one would also see that the zero of energy is displaced from the peak at $(\pi/2,\pi/2)$ by a gap Δ and in addition a small peak disperses away from the Fermi energy as the momentum is increased beyond $(\pi/2,\pi/2)$. An angular resolved bremmstrahlung isochromat spectroscopy (BIS) experiment would show that as $\mathbf{p}$ increases along the diagonal, spectral weight is transferred to an image peak lying symmetrically above the Fermi energy. For a system with only a near-neighbor hopping the spectral weight is evenly divided for $(\pi/2,\pi/2)$ and then shifts heavily to the BIS side as $\mathbf{p}$ increases further. Figures 2(b) and 2(c) show the ω variation of the spectral weight for various values of the momentum $\mathbf{p}$ taken along several additional cuts in the Brillouin zone.

In Fig. 4, the solid points show the position of the peaks in $A(\mathbf{p},\omega)$ versus $\mathbf{p}$. Here the solid curves correspond to the SDW dispersion relation $E_{\mathbf{p}} = \pm\sqrt{\varepsilon_{\mathbf{p}}^2 + \Delta^2}$ for

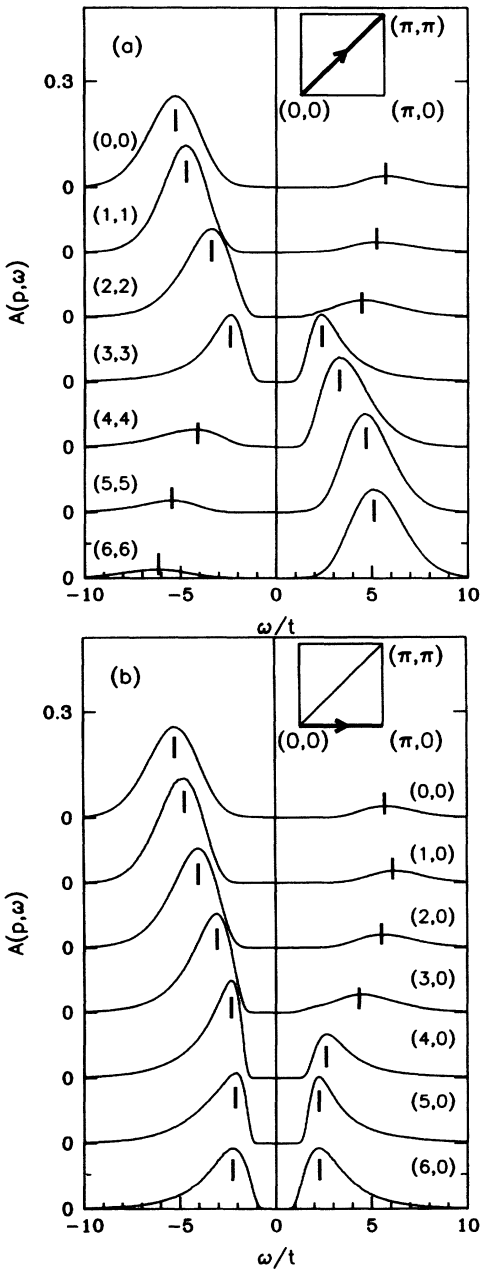

FIG. 2. Single-particle spectral weight $A(\mathbf{p},\omega)$ versus ω for various values of $\mathbf{p}$. The inset in each panel shows the momentum slice through the Brillouin zone. The parameters are the same as in Fig. 1.

$\Delta = 2.4t$, while the dotted line shows $\varepsilon_{\mathbf{p}}$. Note that in the large $U/t \gg 1$ limit, Δ varies as $U/2$ so that

$$E_{\mathbf{p}} = \sqrt{\varepsilon_{\mathbf{p}}^2 + \Delta^2} \simeq \Delta + J(\cos p_x + \cos p_y)^2 \qquad (13)$$

with $J = 4t^2/U$. Thus in this limit, the dispersion only depends upon J. Also in this limit, the kinetic energy of the half-filled band $\langle k_x \rangle$ varies as t^2/U [2] so that the f-sum rule is also set by J.

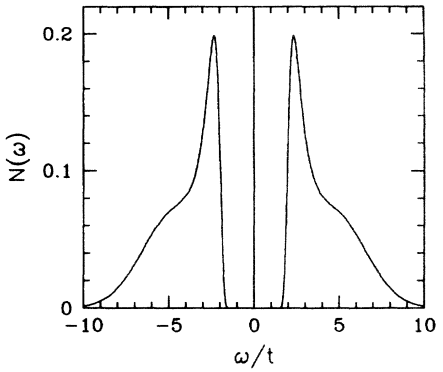

FIG. 3. Single-particle density of states $N(\omega)$.

It appears that the SDW results provide a quite reasonable description of the dispersion of the peaks. In addition, the SDW spectral weight

$$A(\mathbf{p},\omega) = \frac{1}{2}\left(1 - \frac{\varepsilon_{\mathbf{p}}}{E_{\mathbf{p}}}\right)\delta(\omega + E_{\mathbf{p}}) + \frac{1}{2}\left(1 + \frac{\varepsilon_{\mathbf{p}}}{E_{\mathbf{p}}}\right)\delta(\omega - E_{\mathbf{p}}) \qquad (14)$$

provides a natural explanation for the spectal weight transfer found in the Monte Carlo data. In particular, the spectral weight for $\omega \leq 0$ determines the electron momentum distribution

$$\langle n_{\mathbf{p}} \rangle = \int_{-\infty}^{0} d\omega\, A(\mathbf{p},\omega). \qquad (15)$$

In Fig. 5, Monte Carlo results for $\langle n_{\mathbf{p}} \rangle$ are shown as the solid points and the curve corresponds to the SDW result $\frac{1}{2}(1 - \varepsilon_{\mathbf{p}}/E_{\mathbf{p}})$.

Thus it appears that even in the case where U is equal to the bandwidth $8t$, the spin-density-wave picture provides a useful framework for understanding the electronic

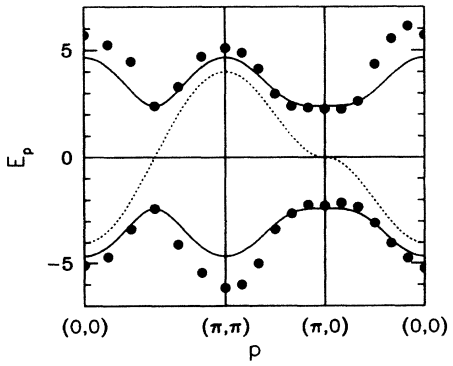

FIG. 4. The solid points correspond to the position $E_{\mathbf{p}}$ of the peaks in $A(\mathbf{p},\omega)$ versus $\mathbf{p}$ for the same parameters as in Fig. 1. The dotted line shows the band structure energy $\varepsilon_{\mathbf{p}} = -2t(\cos p_x + \cos p_y)$, while the solid curves correspond to the SDW result $E_{\mathbf{p}} = \pm(\varepsilon_{\mathbf{p}}^2 + \Delta^2)^{1/2}$.

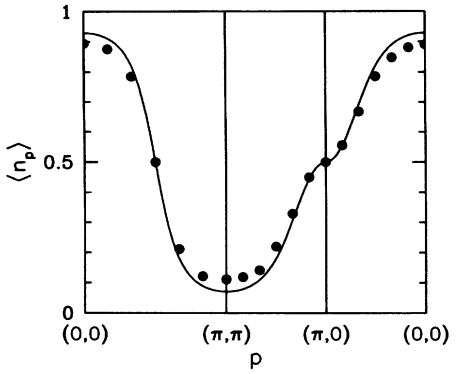

FIG. 5. $\langle n_{\mathbf{p}} \rangle$ versus momentum. The solid points are obtained from the Monte Carlo data by integrating $A(\mathbf{p}, \omega)$ over ω according to Eq. (15). The curve represents the mean field result $\frac{1}{2}(1 - \varepsilon_{\mathbf{p}}/E_{\mathbf{p}})$.

properties of the half-filled insulating state of the Hubbard model. In particular, it provides a reasonable description of $\sigma_1(\omega)$ and the insulating nature of the system. Furthermore, it gives a single-particle spectral weight which disperses in the same way as the Monte Carlo data and in addition exhibits the same shift in the relative spectral weights of the peaks [8].

We thank Z.-X. Shen for useful discussions. N. B. would like to acknowledge support by the National Science Foundation (DMR 91-20000) through the Science and Technology Center for Superconductivity, and D. J. S. would like to acknowledge support for this work from the Department of Energy under Grant No. DE-FG03-85ER45197. S. R. W. would like to thank the office of Naval Research for support under Grant No. N00014-91-J-1143. The numerical calculations reported in this paper were performed at the San Diego Supercomputer Center.

[1] J. R. Schrieffer, X. G. Wen, and S. C. Zhang, Phys. Rev. B **39**, 11 663 (1989).

[2] S. R. White, D. J. Scalapino, R. L. Sugar, E. Y. Loh, J. E. Gubernatis, and R. T. Scalettar, Phys. Rev. B **40**, 506 (1989).

[3] For a recent review of the Monte Carlo technique used here see D. J. Scalapino, in Proceedings of the Summer School on Modern Perspectives in Many-Body Physics, Canberra, January 1993 (World Scientific, Singapore, to be published).

[4] R. N. Silver, D. S. Sivia, and J. E. Gubernatis, Phys. Rev. B **41**, 2380 (1990).

[5] S. R. White, Phys. Rev. B **44**, 4670 (1991); **46**, 5678 (1992); M. Vekic and S. R. White, *ibid.* **47**, 1160 (1993).

[6] D. J. Scalapino, S. R. White, and S. C. Zhang, Phys. Rev. Lett. **68**, 2830 (1992); Phys. Rev. B **47**, 7995 (1993).

[7] The broadening of $0.5t$ used in plotting the SDW results provides a rough estimate of the temperature and frequency dependent quasiparticle lifetime which varies from $T = 0.125t$ to of order t as ω increases. The resolution of the analytic continuation also varies with frequency and ranges from $\sim(0.25-0.5)t$ at low ω to $(1-2)t$ at higher frequencies.

[8] In order to compare theory with experiment we have also carried out Monte Carlo calculations for a Hubbard model with a next-near-neighbor hopping t'. Within the SDW framework this simply alters $\varepsilon_{\mathbf{p}}$ by adding a term $-4t' \cos p_x \cos p_y$. Calculations of the quasiparticle lifetimes due to fluctuations of the sublattice magnetization are also being carried out. The results will be presented in a longer paper.